Turk J Phys
36 (2012) , 253 – 259.

doi:10.3906/fiz-1105-17

Behavior of temperature dependence of permeability curves at different stages of crystallizations of nanocrystalline $Fe_{70.5}Cr_3Cu_1Nb_3Si_{13.5}B_9$

Saadni ISLAM[1], Kazi Hanium MARIA[1], Shamima CHOUDHURY[1], Mohammad Abdul HAKIM[2] and Dilip Kumar SAHA[2]
[1] *Department of Physics, University of Dhaka, Dhaka-1000, BANGLADESH*
[2] *Materials Science Divisions, Atomic Energy Centre, Dhaka-1000, Dhaka-BANGLADESH*
e-mail: kazimaria@univdhaka.edu

Received: 25.05.2011

Abstract

Nanocrystalline amorphous ribbons of composition $Fe_{70.5}Cr_3Cu_1Nb_3Si_{13.5}B_9$ prepared by rapid solidification technique have been studied in the present work. Amorphicity of the ribbons has been confirmed by X-ray diffraction. Crystallization temperatures were identified by X-ray diffraction and crystallization products were analyzed by XRD. When annealed below the crystallization temperature, i.e. when the sample is in amorphous state, temperature dependence of permeability curves were characterized by sharp increase of permeability and subsequent fall to lower value near ferro-paramagnetic transition temperature, which is typical Hopkinson effect for soft ferromagnetic single phase material. Under devitrification, when the sample is in a two phase state, the sharpness of the descent to lower values of permeability is smeared out. This smearing effect is caused by distribution of the Curie temperature of the Fe-depleted residual amorphous matrix. During heating and cooling, it has been observed from a graph of $\mu'(T)$ that the value of permeability and T_C at cooling had increased slightly faster than the heating due to relaxation of the sample. Above the crystallization temperature, we noticed that the heating and cooling curve of $\mu'(T)$ are almost superimposed.

Key Words: Nanostructured alloys, Finemet, soft magnetic properties, XRD, permeability

1. Introduction

The Fe-Cu-Nb-Si-B alloys (i.e. FINEMET) have attracted much interest because of their excellent soft magnetic properties due to particles of α-Fe(Si) dispersed in a residual amorphous matrix [1–4]. This alloy is derived from the conventional Fe-Si-B system with minor additions of copper (Cu) and niobium (Nb). In this case, Cu acts as a nucleating agent whereas Nb inhibits the grain growth of the FeSi phase that crystallizes from the amorphous matrix during annealing. FINEMET exhibits excellent permeability, a low

saturation magnetostriction and a high saturation magnetization which finds use in electric power applications such as transformer cores and other inductive devices. The FeSiB alloy loses its soft magnetic properties when it is crystallized, but the soft magnetic properties of FINEMET alloys are significantly improved due to precipitation of the nanocrystalline phase. The magnetic softness of FINEMET alloy mainly arises from the dispersion of ultrafine grains in an amorphous matrix which reduces the effective magnetic anisotropy (K_{eff}) and magnetostriction (λ_s). This indicates that the exchange interaction between the nanocrystalline and amorphous phases also plays an important role in achieving good soft magnetic properties [5, 6]. The FINEMET alloys are prepared by the rapid solidification technique followed by annealing at elevated temperatures to achieve a nanocrystalline structure. The scope of the present work is to investigate the magnetic interactions between the nanocrystalline and the residual amorphous phases. In this paper, typical magnetic properties of Fe-Cu-Nb-Si-B alloys, which showed excellent soft magnetic properties, are reported.

2. Experimental

Amorphous alloys in the form of ribbons have been prepared with the nominal composition $Fe_{70.5}Cr_3Cu_1Nb_3Si_{13.5}B_9$ by the rapid solidification technique. The ribbons are on average 6 mm wide and 20–25 μm thick. The amorphosity of the ribbons has been confirmed by PW 3040-X Pert Pro (Phillips) X-ray diffractometer with Cu-$K_\propto$ radiation. Temperature dependence of initial permeability of the as-cast and annealed ribbons is measured using a laboratory built furnace and Wayne Kerr 3255 B impedance analyzer.

3. Results and discussions

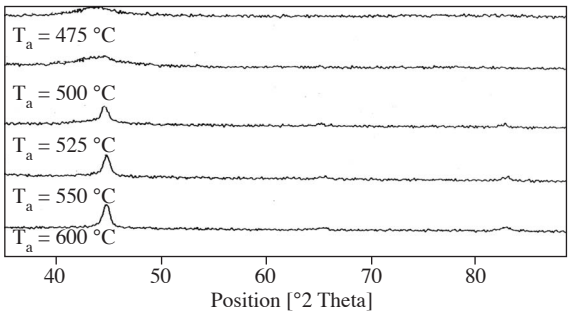

Figure 1. XRD patterns of $Fe_{70.5}Cr_3Cu_1Nb_3Si_{13.5}B_9$ alloy at different annealing temperature for 30 minutes.

X-ray diffraction pattern of the $Fe_{70.5}Cr_3Cu_1Nb_3Si_{13.5}B_9$ samples annealed at 475 °C, 500 °C, 525 °C, 550 °C and 600 °C for 30 minutes are shown in Figure 1. It is observed that, no sharp peak is found at temperature 475 °C and 500 ° C. For the sample annealed at or above 525 °C it is clearly evident that the bcc Fe(Si) peaks become narrower, sharper with greater intensity with increasing annealing temperature, indicating that the crystallite sizes are gradually growing larger. X-ray pattern of T_a = 525 °C, clearly confirms the presence of crystalline phase identified as a bcc α-Fe(Si) solid solution developed in the amorphous matrix.

Figure 2(a) shows the variation of lattice parameter of samples annealed for 30 minutes with varying annealing temperature. With increase in annealing temperature, lattice parameter decreases, assuming negligible peak shift due to stacking fault as in general no peak is observed experimentally. The lattice parameters of bcc α-Fe(Si) phase at different annealing conditions are smaller than the lattice parameter of pure Fe, the

value of which is 2.866 Å. Thus it can be assumed that the decrease of lattice parameter is due to increase of Si content in the Fe(Si)grains as the annealing temperature increases due to contraction of α-Fe lattice. As a result of diffusion of the Silicon with smaller atomic size into the iron lattice with larger atomic size forming a substitution solid during the crystallization process to form α-Fe(Si).

Silicon content of the Fe(Si) nanograins was calculated from the established quantitative relationship between lattice parameter and Si-content in Fe-Si alloys by Bozorth [7]. Si contents in Fe(Si) nanograins created at various annealing temperature have been shown in figure 2(b). This result is compatible with those reported for similar composition [8]. It is observed from the Figure 2(b) that the Si content of α-Fe(Si) increases with increase of annealing temperature attaining maximum value 22.6 at% at $T_a = 600$ °C for annealing time, $t_a = 30$ minutes. The maximum value of 22.6 at% Si is compatible with 23% Si obtained by Mossbauer study [9].

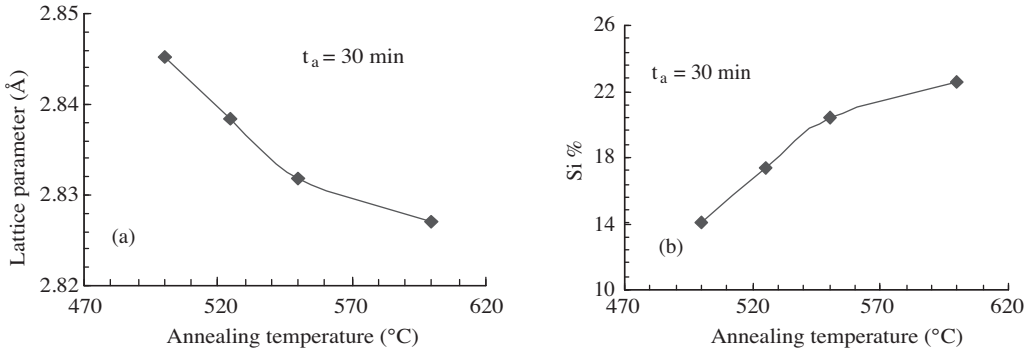

Figure 2. (a) Variation of Lattice parameter With different annealing temperature at Annealing time 30 minutes. (b) Variation of Si% with different annealing temperature at annealing time 30 minutes.

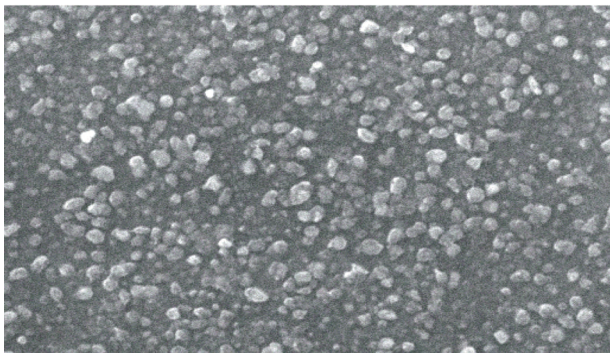

Figure 3. Microstructure by Scanning Electron Microscope of FINEMET alloy.

The annealed alloy "FINEMET" is composed of an ultra-fine grain structure and the microstructure of it is shown in Figure 3. These grains are composed of bcc Fe solid solution and their diameter is about 15 nm.

Figure 4(a) shows the variation of initial permeability, μ' with temperature for the as-cast and samples annealed at 425 °C–475 °C at the fixed frequency of 10 kHz. From X-ray diffraction, no crystalline phase was observed in this range of annealing temperature. The as-cast and annealed samples at 425 °C, permeability is independent of temperature which suddenly decrease toward zero due to ferro-paramagnetic phase transition of amorphous state. For those samples annealed at 450 °C to 525 °C, permeability gradually increased with

temperature and passed through a maximum followed by a sharp fall to near zero with the manifestation of Hopkinson effect characterizing the ferro-paramagnetic transition of the amorphous phase. This is to note that the sharp fall of permeability at the Curie temperature of the amorphous phase clearly indicates the good homogeneity of the amorphous state of the prepared samples. It is also observed from the present study that an enhancement of Curie temperature of the annealed samples up to $T_a = 475$ °C takes place. Enhancement of Curie temperature occurs because of irreversible structural relaxation like long range internal stress, topological and chemical short range order. Further from the analysis of the Mossbauer spectra for the quenched and annealed samples below the crystallization temperature, it has been observed that this treatment leads to the increase in packing density of atoms [10]. Increase in packing density of atoms might have significant contribution in the enhancement of Curie temperature in the amorphous state.

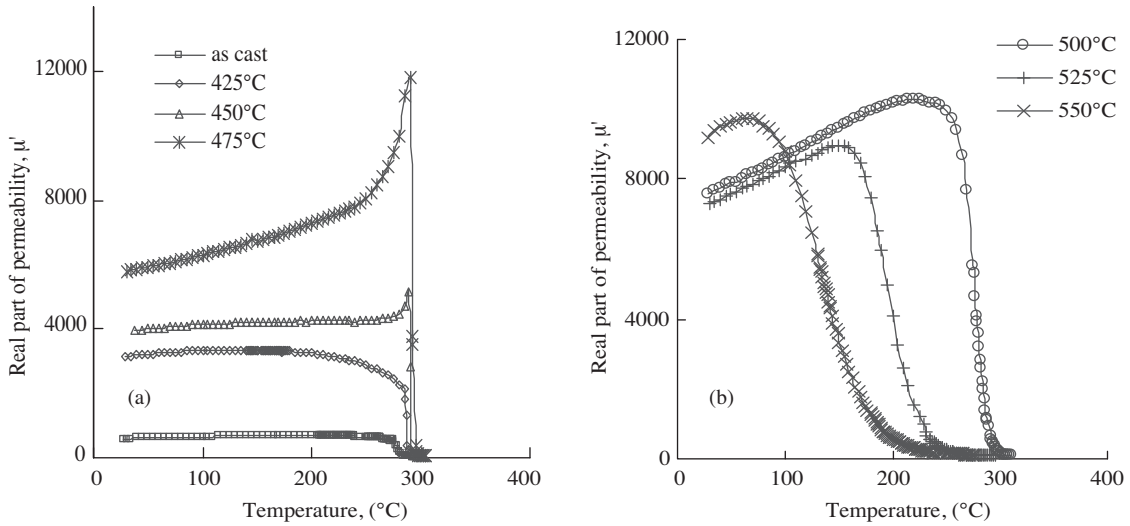

Figure 4. (a, b) Variation of the real part of initial permeability as a function of temperature annealed at different temperature for 30 minutes.

When the annealing temperature is increased above the crystallization temperature i.e. 500 °C, 525 °C and 550 °C, a decrease of Curie temperature with the annealing temperature is observed in Figure 4(b) and the sharpness of the fall to lower values of permeability is progressively smeared out with the appearance of a tail in the high temperature region. These results are in good agreement with those previously reported for the FINEMET composition [11, 12]. Above the crystallization temperature, Curie temperature of the amorphous matrix decreases significantly. The probable reason of decreasing the Curie temperature of the amorphous phase when annealed at and above the crystallization temperature is that the amorphous matrix is depleted with iron and the relative amount of Cr and Nb in the amorphous matrix increases, which weakens the exchange interaction resulting in a decrease of Curie temperature of the amorphous matrix. At higher measuring temperature above T_c^{am} the super-paramagnetic and super ferromagnetic behavior is observed depending on the size and volumetric fraction of crystalline phases and the separation between the crystallites. But in our experiment we did not observed that. Table shows the Curie temperature of FINEMET alloy annealed at different annealing temperature.

$Fe_{70.5}Cr_3Cu_1Nb_3Si_{13.5}B_9$ ribbon has been prepared in the amorphous state. It is known that the amorphous state is metastable. Therefore during the measurement of temperature dependence of permeability relaxation, initiation of crystallization may occur during continuous heating of the specimen, especially when the

Table 1. Curie temperature at different annealing temperatures.

Annealing temperature T_a	Curie temperature T_C
as cast	
425 °C	276 °C
450 °C	285 °C
475 °C	290 °C
500 °C	292 °C
525 °C	270 °C
550 °C	185 °C
276 °C	115 °C

temperature is closer to the crystallization onset temperature. Figure 5(a) shows the $\mu'(T)$ curve of amorphous sample during heating where a sharp fall of permeability at 276 °C corresponding to ferro-paramagnetic phase transition temperature T_c of the amorphous state of the sample is observed. During cooling T_c was found to be 288 °C which is 12 °C higher than that of heating. It is also observed from $\mu'(T)$ graph during heating

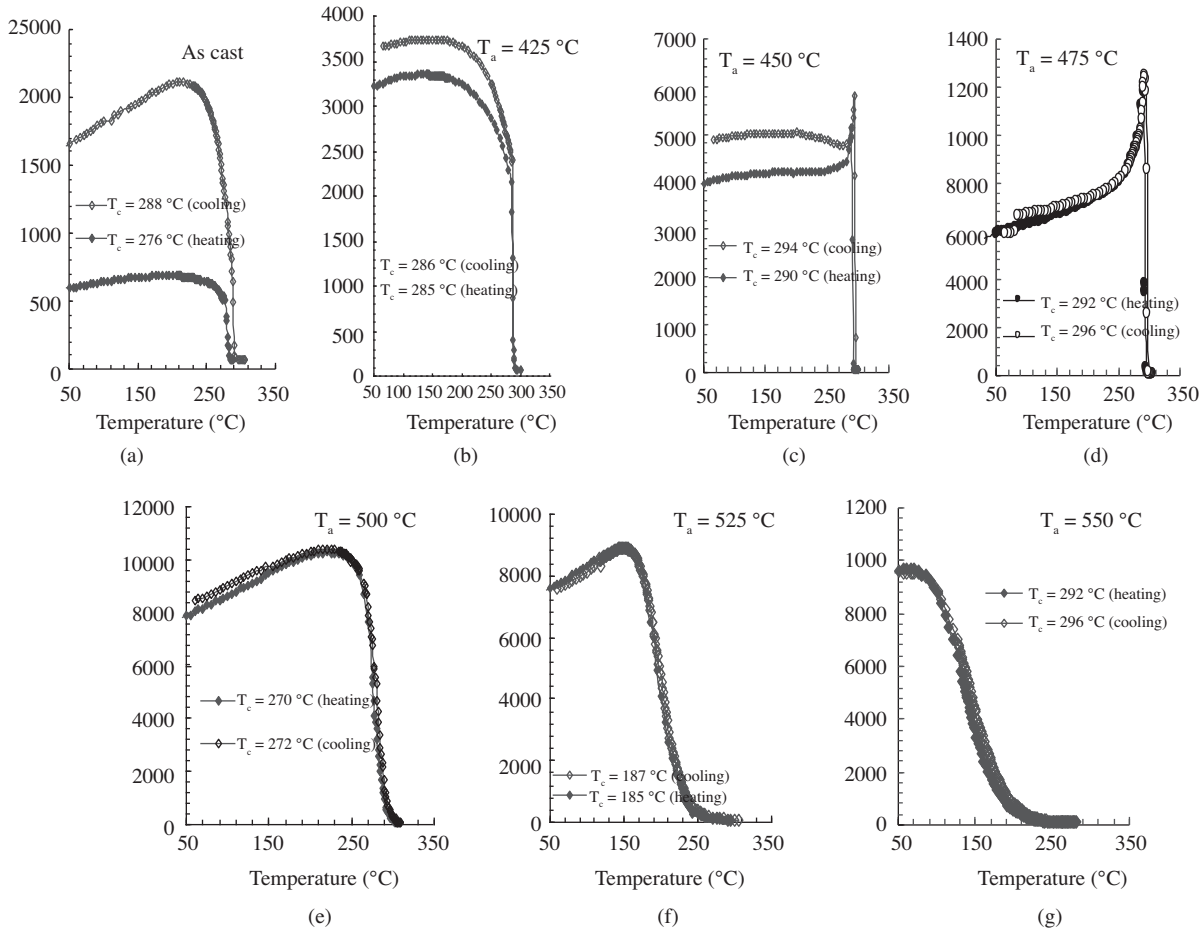

Figure 5. (a, b, c, d, e, f, g) Permeability and ferromagnetic phase transition for sample annealed at different annealing temperatures during heating and cooling.

cooling that a value of permeability at cooling has increased substantially than the heating. This change of T_c and μ' can be explained as a result of relaxation of the amorphous sample. The relaxation includes structural relaxation such as long-range internal stress, topological and chemical short-range order.

From Figures 5(b), (c) and (d), it is observed that difference between the Curie temperature of the sample during heating and cooling does not noticeably differ in contrast with Figure 5(a). Since these samples are annealed at T_a = 425 °C, 450 °C and 475 °C prior to measurement, it may be assumed that necessary relaxation at these temperatures during an isothermal annealing of 30 minutes is sufficient for the relaxation process to come to an end. Therefore insignificant difference between the Curie temperatures during heating and cooling (3 °C to 4 °C) cannot be attributed to any irreversible component of relaxation. Rather, it can be attributed to the thermal hysteresis during heating and cooling along with the complexity of domain formation. During cooling in which case zero anisotropy above the T_c and the subsequent cooling to low temperature is an important parameter to be considered. From these graphs, it is also observed that the enhancement of the permeability during cooling is not that much significant as in the case of Figure 5(a) i.e. amorphous state. The small increase in permeability during cooling may be attributed to the anisotropy compensation with temperature along with the effect of applied AC field. We would like to mention that this small enhancement of μ' does not reflect of the relaxation. From Figures 5(a) to 5(d), it is also noticed that at the T_c, fall of permeability is quite sharp which necessarily indicates homogeneity of the amorphous phase of our sample.

Figures 5(e), (f) and (g) show the permeability annealed at T_a = 500 °C, 525 °C, 550 °C, respectively. If these annealing temperatures are compared with the XRD data on the annealing samples, it is clear that these annealing temperatures are equal to or higher than the temperature of initiation of crystallization which was found to be 500 °C by X-ray diffraction, and it means that the amorphous state of the material no longer exists, which means that the matrix of the sample consists of amorphous + crystallites state, i.e., heterogeneous phase [13].

From Figures 5(e)–(g) we notice that the heating and cooling curve of $\mu'(T)$ almost superimposed each other with insignificant no divergence throughout the entire range of measured temperature. It is also noticed from these curves that the shape of the $\mu'(T)$ is big different than those of Figure 5(a)–(d), which were annealed below 500 °C, the onset of crystallization. Here, it is observed that the permeability at T_c is not sharp, but rather smeared at the Curie temperature. This indicates that the amorphous state is no longer homogeneous since the composition of the amorphous phase may vary at different section of the sample. Accurate determination of T_c from these curves is not that straightforward. Therefore the values of T_c of these samples were determined from the numerical derivative of the data in which T_c has been taken as the temperature where $d\mu'/dt$ attains maximum value. It is also observed from these curves that as the annealing temperature increases the determination of T_c become more crucial, since they display a more diffused nature due to enhancement of heterogeneity and compositional gradient in the remaining amorphous matrix [14].

4. Conclusions

Nanocrystalline alloys in the form of thin ribbons with the nominal composition of $Fe_{70.5}Cr_3Cu_1Nb_3Si_{13.5}B_9$ have been prepared by rapid solidification technique. The presence of 3% of Cr substitution on Fe, 1% of Cu and 3% of Nb on Fe-Si-B alloys changed the crystallization process considerably. After annealing, Fe(Si) nanometric crystallites with grain size of 15 nm grow in the residual amorphous matrix. The formation of this particular nanostructure was ascribed to the combined effect of Cr, Cu, and Nb. Curie temperature

samples increase with the increasing annealing temperature due to the irreversible structural relaxation like long range internal stress, topological and chemical short range order. It has also been observed from $\mu'(T)$ graph of amorphous sample during heating and cooling that the value of permeability and T_c at cooling had increased slightly than the heating because of relaxation of the amorphous sample. Above the crystallization temperature we noticed that the heating and cooling curve of $\mu'(T)$ is almost superimposed.

Acknowledgments

The authors are thankful to Materials Science Division, Atomic Energy Centre, Dhaka- 1000, Bangladesh for extending the use of experimental facilities

References

[1] Y. Yoshizawa, S. Oguma, K. Yamauchi, *J. Appl. Phys.*, **64**, (1988), 6044.

[2] G. Herzer, *IEEE Trans. Magn.*, **25**, (1989), 3327.

[3] Y. Yoshizawa, K. Yamauchi, *Mater. Trans. Jpn. Int. Metals*, **31,** (1990), 307.

[4] G. Herzer, H. Warlimont, *Nanostruct. Mater.*, **1**, (1992), 263.

[5] K. Y. He, J. Zhi, L. Z. Cheng, M. L. Sui, *Mater. Sci. Eng. A*, **181**, (1994), 880.

[6] F. Zhou, K. Y. He, K. C. Bai, *J. Appl. Phys.*, **80**, (1996), 5209.

[7] R. M. Bozorth, Ferromagnetism, vol 217, (D. Van Nostrand Company, Inc Princeton, NJ, 1964), p. 74.

[8] K. Brzòzka, A. lawska-Waniewska, M. Gawroski, K. Jezuita and H. K. Lachowicz, *J. Magn. Magn. Mater*, **140**, (1995), 481.

[9] V. Franco, C. F. Conde, A. Conde, *J. Magn. Magn. Mat.*, **185**, (1998), 353.

[10] A. Bachowicz, J. Zbroszczyk, J. Olszewski, W. H. Ciurzyska, H. Fukunaga, K. Narita, B. Wysocki, M. Hasiak, *J. Mag. Mag. Mater.*, **215**, (2000), 422.

[11] V. Franco, C. F. Conde., A. Conde, L. F. Kiss, *J. Magn Magn. Mater.*, **215**, (2000), 400.

[12] S. N. Kane, S. Sarabhai, Ajay Gupta, L. K. Varga and T. Kulik, *J.Magn.Magn.Mater.*, **215**, (2000), 372.

[13] C. Miguel, S. Kaloshkin, J. Gonzalez and A. Zhukov, *J. Non-Cryst. Solid.,* **329**, (2003), 63.

[14] H. Bohnel, G. Mclntosh and G. Sherwood, *Physics and chemistry of the Earth.*, **27**, (2002), 1305.